

Gap soliton and quasi-linear 2π pulse in continuous resonant photonic crystals

Lidiya V. Frolova,* Alexander A. Skorynin, and Boris I. Mantsyzov

*Department of Physics, M. V. Lomonosov Moscow State University,
Moscow 119991 Russia*

**Corresponding author: lidiya.frolova@gmail.com*

Received April 23, 2013; revised June 22, 2013; accepted June 23, 2013;
posted June 24, 2013 (Doc. ID 189193); published July 24, 2013

Nonlinear interaction of coherent intensive optical radiation with continuous resonant photonic crystal (RPC) is analytically and numerically studied in the framework of semiclassical approach using the two-wave Maxwell–Bloch equations. The analytical solution being the gap soliton of self-induced transparency is obtained in the case of an initially unexcited continuous RPC. This solution is confirmed numerically. Influence of both initial inversion and resonant atom concentration function profile on the pulse dynamics in continuous RPC is analyzed. Suppression of the Bragg reflection and a “quasi-linear” 2π pulse propagation in the case of zero initial inversion in continuous RPC is shown. The possibility of laser pulse compression using slow spatial changing of resonant atom concentration is demonstrated. © 2013 Optical Society of America

OCIS codes: (270.5530) Pulse propagation and temporal solitons; (270.1670) Coherent optical effects; (050.5298) Photonic crystals.

<http://dx.doi.org/10.1364/JOSAB.30.002240>

1. INTRODUCTION

Taking into account nonlinearity in the interaction of electromagnetic waves with periodic media, or photonic crystals (PC), allowed for significant change to the current conceptions of solitary wave propagation dynamics in such structures [1–3]. It was shown that within the linear photonic band gap there can propagate nonlinear solitary waves, so called gap solitons, in photonic crystals with different types of nonlinearity: resonant [4–8], cubic [9–13], and quadratic ones [14,15]. The trapped gap solitons with amplitudes less than freely propagating pulse amplitude can oscillate inside a PC [16,17] and interact with exact solitons inelastically [18–20]. Essential part of these results [4–8,16–20] was obtained during a study of the discrete resonant photonic crystals (RPCs) model [4], a so-called resonant Bragg grating, where resonant two-level atoms are localized in periodically situated thin layers divided by homogeneous or periodic linear dielectric medium. This model of the δ -function nonlinear grating allowed for the obtaining of simple analytical solutions of some difficult nonlinear dynamic problems, but for the analysis of experimental data we need more realistic model. A relevant model is a continuous RPC, that is, the structure with the periodic continuous function of resonant atom concentration; for example, PC made of porous glass [21,22] filled with a gas of resonant two-level atoms. Optical phenomena in such media for the present are poorly studied. Only one particular case of continuous RPC with harmonic modulation of resonant atom concentration was considered [23]. It was shown theoretically that, in this structure, propagation of the gap solitons of self-induced transparency (GS SIT) is allowed. Nevertheless, in a continuous RPC, qualitatively new effects can be expected. It is actually well known that, under conditions of incoherent light–matter interaction in the

homogeneous resonant medium, a refraction index becomes equal to the linear matrix refraction index if the initial value of inversion is equal to zero [24]. It means that, in this case, resonant atoms do not influence the dynamics of pulse propagation as if they were absent in the medium. In a continuous RPC the effect is similar but, in the coherent case, it should lead to suppression of the Bragg reflection because the reason for the Bragg reflection in such media is periodicity of function of resonant atom concentration.

In this paper, we consider interaction of coherent intensive optical radiation with continuous RPC having rather arbitrary distribution of two-level atom concentration in the framework of the semiclassical approach. Through analytical solving of the set of the two-wave Maxwell–Bloch (MB) equations, the existence of the GS SIT in the general case of a continuous RPC with an arbitrary concentration function is shown. The pulse formation process in a continuous RPC is studied and it is also shown that the initial inversion and resonant atom concentration profile can have a significant effect upon intensive pulse propagation dynamics. So, in the case of zero initial inversion in a continuous RPC, the propagation of a so called “quasi-linear” 2π pulse takes place. The pulse interacts nonlinearly and coherently with each two-level atom, but average medium polarization is zero because of spatial phase mismatching between atom dipole moments and field wave. As a result, the pulse propagates with group velocity determined by the linear matrix medium only. In structures with slowly changing resonant atom concentration profiles, essential increase of intensity and compression of soliton-like pulses might be done. The argumentation of this effect appearance is given; compression occurs because of energy transfer from backward wave to passing one.

2. TWO-WAVE MAXWELL–BLOCH EQUATIONS AND STATIONARY SOLUTIONS

Let us consider the coherent interaction of a quasi-monochromatic intensive laser radiation pulse with a continuous RPC, which is a homogenous dielectric medium matrix doped with resonant two-level atoms. To solve this problem, we will use a semiclassical description of light–matter interaction—classical field interacts with quantum oscillators. The resonant atom concentration function is assumed to be the continuous periodical one-dimensional function of the coordinate $\rho(x) = \rho(x + d)$ with the period equal to d . The concentration ρ must be small enough to neglect dipole–dipole interaction of resonant atoms and local field effects. Using the Maxwell equation, we obtain the wave equation characterizing propagation of the plane-polarized light along the x axis in this medium,

$$E_{xx}(x, t) - \varepsilon c_0^{-2} E_{tt}(x, t) = 4\pi c_0^{-2} P_{tt}^{\text{NL}}(x, t), \quad (1)$$

where E is the electric field of light wave; P^{NL} is a small resonant polarization, that is, the dipole moment of the unit of the structure volume provided by doping resonant atoms; $\varepsilon = \text{const}$ is the dielectric constant of the homogenous linear matrix; c_0 is the light velocity in vacuum; and the subscripts denote the partial derivatives to x and t . Polarization P^{NL} is defined from solution of Bloch equations for the dipole moment and the inversion of two-level atoms. The central frequency ω is assumed to coincide with the atom-resonant transition frequency, and the resonant grating period d in the case of normal incidence of pulses upon the structure obeys the Bragg condition for the central frequency $2k = mH$ or $d = m\lambda/2$, where $k = \omega/c = 2\pi/\lambda$, $c = c_0/\sqrt{\varepsilon}$ is the light velocity in the unmodulated linear medium, $H = 2\pi/d$ is the modulus of reciprocal lattice vector, and m is an integer, a diffraction order. The satisfaction of the Bragg condition makes it possible to reduce the number of waves passing within the structure to two counterpropagating nonlinear waves strongly coupled with each other, which are called the Bragg waves. Propagation constants of these nonlinear waves $\pm k$ are equal to real parts of effective wave numbers of the linear Bragg modes within the linear photonic band gap $k = mH/2$. Let us suppose that the pulse duration is large enough so its spectrum is entirely localized in the photonic band gap. Then we will seek the solution of the wave equation in the form of two quasi-monochromatic counterpropagating waves with complex, slowly varying amplitudes $E^\pm(x, t)$,

$$E(x, t) = (1/2)(E^+(x, t)e^{i(kx-\omega t)} + E^-(x, t)e^{i(-kx-\omega t)} + \text{c.c.}), \quad (2)$$

where c.c. is the complex conjugate of this expression. The phase change of the waves propagating in a periodic structure, which is taken into account in the Floquet–Bloch theorem by the effective wave vector of Bloch waves, here will be taken into account directly through spatial dependence of complex wave amplitudes $E^\pm(x, t)$.

Then consider equations for slowly varying amplitudes. For this purpose, we substitute the solution in Eq. (2) into Eq. (1) using the slowly varying in time and space envelope approximation

$$|E_x^\pm| \ll |kE^\pm|, \quad |E_t^\pm| \ll |\omega E^\pm|,$$

and get the equation

$$\begin{aligned} & (E_x^+ + c^{-1}E_t^+)e^{i(kx-\omega t)} + (-E_x^- + c^{-1}E_t^-)e^{-i(kx+\omega t)} + \text{c.c.} \\ & = -(4\pi i/kc_0^2)P_{tt}^{\text{NL}}. \end{aligned} \quad (3)$$

To separate amplitudes E^\pm and their complex conjugate $(E^\pm)^*$, it is necessary to multiply Eq. (3) by $\exp(i\omega t)$ and average it over a time $\Delta t \gg \omega^{-1}$ but less than the typical time of amplitudes E^\pm changing, i.e., the pulse duration. Then we multiply Eq. (3) in turn by $\exp(\pm ikx)$ and average it over a volume $V \sim \lambda^3$ to exclude oscillating terms of order $\exp(\pm 2ikx)$. Consequently, we get the following equation for counterpropagating wave field amplitudes:

$$\pm E_x^\pm + c^{-1}E_t^\pm = -(4\pi i/kc_0^2)\langle P_{tt}^{\text{NL}}e^{i\omega t}e^{\mp ikx} \rangle_{\Delta t, V}, \quad (4)$$

where the angular brackets $\langle \dots \rangle_{\Delta t, V}$ denote the averaging over a time Δt and a volume V . The atomic polarization function $P^{\text{NL}}(x, t)$ in Eq. (4) is determined by matter equations of the structure.

Let the period of the structure d exceed considerably the typical distance b between resonant atoms. Then the continuous function of the atomic resonant polarization in the wave Eq. (4) can be written in the form

$$P^{\text{NL}}(x, t) = \frac{P_{\Delta V}(x, t)}{\Delta V} = \frac{P_{\Delta V}(x, t)}{N} \frac{N}{\Delta V} = P'(x, t)\rho(x), \quad (5)$$

where $P_{\Delta V}(x, t)$ is the total dipole moment of resonant atoms in a small volume $b^3 \ll \Delta V \ll d^3$ in the region round the x point and N is the number of resonant atoms in the volume ΔV . $P'(x, t) = P_{\Delta V}(x, t)/N = (1/2)[-i\mu P(x, t)\exp(-i\omega t) + \text{c.c.}]$ is the average over the ensemble of N particles dipole moment of the atom in the x point and μ is the matrix element of the transition dipole moment. The value of the slowly changing in time complex amplitude of the normalized atom dipole moment $P(x, t)$ is obtained from the average over a small volume ΔV Bloch equations [23]

$$\begin{aligned} P_t(x, t) &= n(x, t)[\Omega^+(x, t)e^{ikx} + \Omega^-(x, t)e^{-ikx}], \\ n_t(x, t) &= -\text{Re}\{P^*(x, t)[\Omega^+(x, t)e^{ikx} + \Omega^-(x, t)e^{-ikx}]\}, \end{aligned} \quad (6)$$

where $n(x, t)$ is the inversion averaged over the ensemble of atoms in the x point; $\Omega^\pm(x, t) = (\mu/\hbar)E^\pm$ are the normalized wave amplitudes; $\tau_c = (\hbar\varepsilon/2\pi\mu^2\rho_0\omega)^{1/2}$ is the cooperative time [25], characterizing mean lifetime of the photon in the resonant medium and defining the size of the linear photonic band gap in RPC [4]; ρ_0 is the dimensional modulation amplitude of the concentration of resonant atoms $\rho(x) = \rho_0\tilde{\rho}(x)$; and $\tilde{\rho}(x)$ is the nondimensional periodic function. Then, substituting the expression for the polarization [Eq. (5)] into the equations for slowly varying amplitudes of the counterpropagating waves [Eq. (4)], taking into account that $P(x, t)$ slowly changes in time $|P_t| \ll |\omega P|$ and, jointly with Eq. (6), we get the set of two-wave MB equations for the continuous RPC in nondimensional variables:

$$\pm \Omega_\xi^\pm(\xi, \tau) + \Omega_\tau^\pm(\xi, \tau) = \langle P(\xi, \tau)\tilde{\rho}(\xi)e^{\mp ik\xi} \rangle_\lambda, \quad (7a)$$

$$P_{\tau}(\xi, \tau) = n(\xi, \tau)[\Omega^{+}(\xi, \tau)e^{ik'\xi} + \Omega^{-}(\xi, \tau)e^{-ik'\xi}], \quad (7b)$$

$$n_{\tau}(\xi, \tau) = -\text{Re}\{P^{*}(\xi, \tau)[\Omega^{+}(\xi, \tau)e^{ik'\xi} + \Omega^{-}(\xi, \tau)e^{-ik'\xi}]\}, \quad (7c)$$

where $\Omega^{\pm}(\xi, \tau) = (\tau_c \mu / \hbar) E^{\pm}$ are the nondimensional normalized wave amplitudes; $\xi = x/(c\tau_c)$, $\tau = t/\tau_c$ are the nondimensional space and time coordinates, respectively $k' = 2\pi/\lambda'$, $\lambda' = \lambda/(c\tau_c)$; and the angular brackets denote averaging over the space region $\Delta\xi \sim \lambda'$.

Let us solve analytically the MB Eqs. (7a)–(7c) for the continuous periodic function of resonant atom concentration $\tilde{\rho}(\xi)$ in the case of the initially unexcited medium: $n(\xi; \tau = 0) = -1$. The function $\tilde{\rho}(\xi)$ is represented as the Fourier series

$$\tilde{\rho}(\xi) = \sum_{m=-\infty}^{\infty} C_m e^{imH'\xi}, \quad (8)$$

where $H' = 2\pi/d'$, $d' = d/(c\tau_c)$, $C_m = (1/d') \int_{-d'/2}^{d'/2} \tilde{\rho}(\xi) e^{-imH'\xi} d\xi$ are the Fourier coefficients and $d' = \lambda'/2$ due to the Bragg condition. For the sake of simplicity, we will consider only even functions; then

$$C_m = C_{-m} = (1/d') \int_{-d'/2}^{d'/2} \tilde{\rho}(\xi) \cos(mH'\xi) d\xi.$$

After substituting Eq. (8) into Eq. (7a), we will obtain

$$\pm \Omega_{\xi}^{\pm}(\xi, \tau) + \Omega_{\tau}^{\pm}(\xi, \tau) = \left\langle P(\xi, \tau) \sum_{m=-\infty}^{\infty} C_m e^{ik'\xi(2m\mp 1)} \right\rangle_{\lambda'}. \quad (9)$$

Further, we multiply Eq. (7a) by $\exp(ik'\xi)$,

$$P_{\tau}(\xi, \tau)e^{ik'\xi} = n(\xi, \tau)[\Omega^{+}(\xi, \tau)e^{2ik'\xi} + \Omega^{-}(\xi, \tau)], \quad (10)$$

and then by $\exp(-ik'\xi)$,

$$P_{\tau}(\xi, \tau)e^{-ik'\xi} = n(\xi, \tau)[\Omega^{+}(\xi, \tau) + \Omega^{-}(\xi, \tau)e^{-2ik'\xi}], \quad (11)$$

and average Eqs. (9)–(11) over the space interval $\Delta\xi \sim \lambda'$. Supposing that $n(\xi, \tau)$ slowly changes within this space interval, one neglects the averaged oscillating exponents and eventually obtains the following set of equations:

$$\Omega_{\tau}^{\pm}(\xi, \tau) \pm \Omega_{\xi}^{\pm}(\xi, \tau) = C_1 P^{\pm}(\xi, \tau) + C_0 P^{\mp}(\xi, \tau), \quad (12a)$$

$$P_{\tau}^{+}(\xi, \tau) = n(\xi, \tau)\Omega^{-}(\xi, \tau), \quad (12b)$$

$$P_{\tau}^{-}(\xi, \tau) = n(\xi, \tau)\Omega^{+}(\xi, \tau), \quad (12c)$$

$$n_{\tau}(\xi, \tau) = -\text{Re}[P^{*+}(\xi, \tau)\Omega^{+}(\xi, \tau) + P^{*-}(\xi, \tau)\Omega^{-}(\xi, \tau)], \quad (12d)$$

where $P^{\pm}(\xi, \tau) \equiv \langle P(\xi, \tau)e^{\pm ik'\xi} \rangle_{\lambda'}$, $C_1 = C_{-1} = (1/d') \int_{-d'/2}^{d'/2} \tilde{\rho}(\xi) \cos(H'\xi) d\xi$, and $C_0 = (1/d') \int_{-d'/2}^{d'/2} \tilde{\rho}(\xi) d\xi$.

The introduced quantities P^{+} and P^{-} have the meaning of the averaged atom dipole moments, occurring as the response to the forward and backward Bragg waves respectively; this is

clearly seen from Eqs. (12b) and (12c). Obviously, these quantities characterize the matter polarization.

The obtained set of equations does not contain a spatial averaging operator; therefore, it can be solved analytically without additional approaches. We will search the solution of Eqs. (12) in the form of stationary solitary waves

$$\Omega^{\pm}(\xi, \tau) = \Omega_0^{\pm} \text{sech}\left(\frac{\xi - v\tau}{v\tau_p}\right), \quad (13)$$

where Ω_0^{\pm} are unknown amplitudes of forward and backward waves, v is the pulse velocity normalized to the light velocity in vacuum c , and τ_p is the pulse duration normalized to τ_c .

Let C_1 not equal C_0 . Expressions for $P^{\pm}(\xi, \tau)$ are derived from Eqs. (12a) and (13),

$$P^{\pm}(\xi, \tau) = \pm \frac{C}{v\tau_p} [C_0(1 \pm v)\Omega_0^{\mp} + C_1(1 \mp v)\Omega_0^{\pm}] \text{sech } \varphi \text{th } \varphi, \quad (14)$$

where $C = 1/(C_0^2 - C_1^2)$, $\varphi = (\xi - v\tau)/v\tau_p$. Substituting Eqs. (13) and (14) into Eqs. (12b) and (12c), we obtain the ratio of amplitudes $\alpha = \Omega_0^{-}/\Omega_0^{+}$,

$$\alpha_{1,2} = \frac{-C_0 \pm \sqrt{C_0^2 - C_1^2(1 - v^2)}}{C_1(1 + v)}, \quad (15)$$

depending on velocity v . Taking into account Eqs. (13) and (15) we obtain n and Ω_0^{+} from the Bloch Eqs. (12b)–(12d)

$$n = -\frac{C}{v\tau_p^2} [C_0(1 - v) + C_1\alpha(1 + v)](1 - 2 \text{sech}^2 \varphi), \quad (16)$$

$$\Omega_0^{+} = \frac{2}{\tau_p} \sqrt{\frac{C_0(1 - v) + C_1\alpha(v + 1)}{C_0[1 - v - \alpha^2(1 + v)] + 2C_1\alpha v}}. \quad (17)$$

Using the condition of pulse localization $n(\xi = \pm\infty; \tau) = -1$, we get from Eq. (16)

$$\tau_p^2 = \frac{C}{v} [C_0(1 - v) + C_1\alpha(1 + v)]. \quad (18)$$

Only value $\alpha = \alpha_1$ in Eq. (15) has a physical meaning, because introducing $\alpha = \alpha_1$ into Eq. (18) leads to the physically correct inequality $\tau_p^2 > 0$ whereas, assuming $\alpha = \alpha_2$, we get $\tau_p^2 < 0$. Finally one obtains the following analytical solution:

$$\begin{aligned} \Omega^{\pm} &= \Omega_0^{\pm} \text{sech } \varphi, \\ P^{+} &= \frac{C}{v\tau_p} [C_1(1 - v)\Omega_0^{+} + C_0(1 + v)\Omega_0^{-}] \text{sech } \varphi \text{th } \varphi, \\ P^{-} &= -\frac{C}{v\tau_p} [C_0(1 - v)\Omega_0^{+} + C_1(1 + v)\Omega_0^{-}] \text{sech } \varphi \text{th } \varphi, \\ n &= C \frac{C_0 v - \sqrt{C_0^2 - C_1^2(1 - v^2)}}{v\tau_p^2} (1 - 2 \text{sech}^2 \varphi), \end{aligned} \quad (19a)$$

where

$$\tau_p = \sqrt{\frac{C}{v} \left[\sqrt{C_0^2 - C_1^2(1-v^2)} - C_0 v \right]}, \quad (19b)$$

$$\Omega_0^+ = \frac{2}{\tau_p} \sqrt{\frac{C_0(1-v) + C_1\alpha(v+1)}{C_0(1-v - \alpha^2(1+v)) + 2C_1\alpha v}}, \quad \Omega_0^- = \alpha\Omega_0^+, \quad (19c)$$

$$\alpha = \frac{\sqrt{C_0^2 - C_1^2(1-v^2)} - C_0}{C_1(1+v)}. \quad (19d)$$

In spite of the fact that wavelength precisely satisfies the Bragg condition, the solution (19) presents the stationary solitary wave which propagates through the structure keeping its amplitude, profile, and velocity. The obtained solution thus corresponds to the GS SIT in the continuous RPC with an arbitrary function of resonant atom concentration.

It results from Eqs. (19b)–(19d) that $\lim_{v \rightarrow 0} \Omega_0^\pm \rightarrow 0$, i.e., in the case of an even periodic function of atom concentration $\tilde{\rho}(\xi)$, the set of two-wave MB equations does not have the zero-velocity solution in the form of the standing soliton existing in the discrete resonant grating [4]. It is to be expected that pulses propagating with small velocities in the medium with such function $\tilde{\rho}(\xi)$ would be unstable.

Note that retaining in Eq. (12a) by averaging only terms including the Fourier coefficients C_0 , C_1 , and C_{-1} , we in fact reduce any periodic even function $\tilde{\rho}(\xi)$ to the form $\tilde{\rho}(\xi) = C_0 + 2C_1 \cos H'\xi$, $H' = 2k'$, so implying that the Fourier coefficients of higher orders C_m , $|m| \geq 2$, give a negligible contribution into the analytical solution. To find out to what extent this supposition is valid, we have performed the direct numerical integration of the two-wave MB Eqs. (7), followed by comparison of analytical and numerical solutions.

At numerical solving of the two-wave MB Eqs. (7), the function of resonant atom concentration in the structure was taken as $\tilde{\rho}(\xi) = (1 + \cos^3 2k'\xi)/2$. In Figs. 1(a) and 1(b), the analytically calculated dependencies of the pulse amplitudes Ω_0^\pm on the pulse velocity v are shown by solid lines. The amplitudes are normalized to the values Ω_0^\pm at $v = 0.92$. The circles indicate values of the normalized amplitudes obtained by numerical solving of the MB equations under the following initial and boundary conditions:

$$\begin{aligned} \Omega^\pm(\xi; \tau = 0) &= 0, P(\xi; \tau = 0) = 0, n(\xi; \tau = 0) = -1, \\ \Omega^+(\xi = 0; \tau) &= \Omega_0^+ \operatorname{sech} \varphi, \Omega^-(\xi = L; \tau) = 0, \end{aligned} \quad (20)$$

where L is the nondimensional length of the resonant structure. Numerical simulation was carried out with the method of characteristics. The figures show good coincidence of the analytical and numerical solutions in the case of large pulse velocities. The gap soliton of SIT is formed in the structure very quickly at the depth about pulse length. This effect is well seen from Figs. 1(c) and 1(d), where formation and propagation of gap solitons are shown. Nevertheless, a natural question arises why the values Ω_0^\pm obtained numerically at velocities $v < 0.8$ do not coincide with the analytical results at the same velocities.

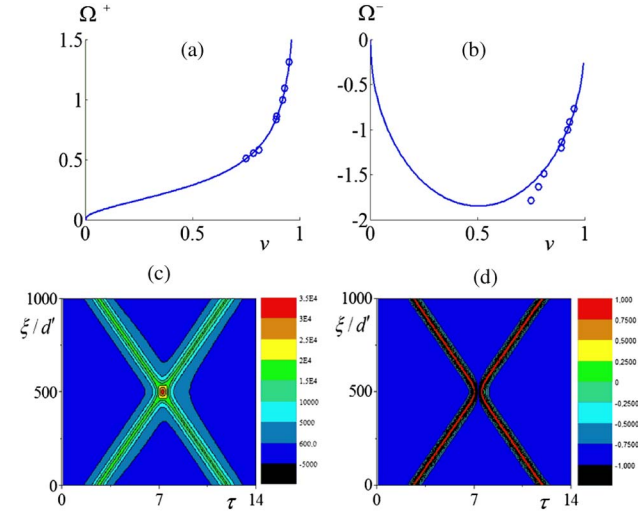


Fig. 1. Dependencies of amplitudes of (a) forward Ω^+ (arb. units) and (b) backward Ω^- (arb. units) waves on pulse velocity v . Continuous lines show dependencies calculated from formulas in Eq. (19); circles show values of amplitudes, obtained through numerical integration of the MB Eqs. (7). (c) Dynamics of the sum of amplitudes $\Omega^+ + \Omega^-$ of two counterpropagating gap solitons with equal velocities $v = 0.95$, and (d) corresponding inversion of resonant atoms n .

As mentioned previously, the absence of a zero-velocity solution of the set of two-wave MB equations gives evidence of possible instability of pulses propagating with small velocities. The numerical solution is actually unstable at $v < 0.8$ [corresponding circles in Fig. 1(b)]. In Figs. 1(a) and 1(b), the values of stable pulse amplitudes at $v \geq 0.8$ are demonstrated.

Note that the Fourier coefficients C_1 and C_0 are equal to each other only for the profile of concentration of resonant atoms having a form of a grating of δ -functions, that is, the discrete RPC. In this case, Eqs. (12) are inapplicable because averaging of the right-hand part of Eq. (7a) results in the equation in the form $P_\tau(\xi, \tau) = n(\xi, \tau)[\Omega^+(\xi, \tau) + \Omega^-(\xi, \tau)]$ [4], replacing Eqs. (12b) and (12c). In a discrete RPC, a slow gap soliton can be stable at a low velocity down to zero velocity [4,16].

We will next show that through changing parameters of the structure, namely the initial inversion and the profile of resonant atom concentration, one can control pulse dynamics and their parameters.

3. PULSE DYNAMICS CONTROL USING INITIAL EXCITATION OF THE RESONANT MEDIUM AND CHANGING OF THE ATOM CONCENTRATION PROFILE

To analyze influence of initial inversion population value on the propagating pulse dynamics in the continuous RPC, numerical integration of the set of MB Eqs. (7) was carried out for two cases: initially unexcited medium with inversion $n(\xi; \tau = 0) \equiv n_0 = -1$ and medium with zero initial inversion $n_0 = 0$. In the first case, the initial and boundary conditions are described by Eq. (20); for the second case, we take the conditions

$$\begin{aligned} \Omega^\pm(\xi; \tau = 0) &= 0, P_1(\xi; \tau = 0) = 0, \\ P_2(\xi; \tau = 0) &= 1, n(\xi; \tau = 0) = 0, \\ \Omega^+(\xi = 0; \tau) &= \Omega_0^+ \operatorname{sech} \varphi, \Omega^-(\xi = L; \tau) = 0, \end{aligned}$$

where $P_1 = \text{Re} P$, $P_2 = \text{Im} P$. Input pulse amplitudes and durations were selected such that the pulse area would be equal to 2π . The atom concentration was selected in the form $\tilde{\rho}(\xi) = (1 + \cos 2k'\xi)/2$.

The results of numerical integration are shown in Figs. 2(a)–2(c). The incident pulse amplitudes are the same in both cases $n_0 = -1$ and $n_0 = 0$ [Fig. 2(a)]. In Figs. 2(b) and 2(c), one can see that the backward wave amplitudes differ dramatically. The forward and backward wave dynamics in the first case correspond to the GS SIT with velocity $v = 0.94$. In the second case, the backward wave amplitude $\Omega^-(\xi = 0; \tau)$ is negligibly small in comparison with the corresponding incident wave amplitude $\Omega^+(\xi = 0; \tau)$ and the amplitude of the backward wave forming in the case of initially unexcited atoms $n_0 = -1$. Within the structure, the pulse forms and the values of the amplitudes are similar to that shown in Fig. 2. This result indicates that, at the boundary and in the bulk of the structure, the suppression of both the total Bragg reflection and photonic band gap occurs if $n_0 = 0$. Consequently, a pulse in a resonant periodic structure does not slow down like the gap soliton but propagates in the same way as pulses in a linear homogenous medium, namely with the velocity equal to light velocity in the linear matrix.

The pulse propagating in the structure includes the field Ω^+ of the forward wave and atom excitation. The backward wave Ω^- in the structure does not exist. Thereby, under fixed initial conditions $n_0 = 0$, the Bragg reflection is suppressed and energy exchange occurs only between the propagating wave and resonant atoms of the structure. The appearance of this effect is due to fundamental difference between the spatial distribution of the mean atom dipole moment and inversion in this case and those in the case of initially unexcited medium (Fig. 3). Actually, Eq. (7b) shows that, at $n_0 = -1$ and $P(\xi; \tau = 0) = 0$, the changing rate of dipole moment P_τ is large and therefore field Ω^+ imposes its phase $k'\xi$ on the dipole moment $P(\xi, \tau)$. Then inversion $n(\xi, \tau)$ will be a slowly varying function in space [Eq. (7c)]. On the contrary, in the case of initial conditions $n_0 = 0$ and $P(\xi; \tau = 0) = 1$, field Ω^+ imposes its space phase $k'\xi$ on inversion $n(\xi, \tau)$ [Eq. (7c)]. In this case, $P(\xi, \tau)$ oscillates in space with a doubled frequency as $\exp(2ik'\xi)$ [Eq. (7c)]. This leads to zero average polarization in right-hand part of Eq. 7(a) and to zero response of resonant structure. It is shown below that the obtained numerical results coincide well with the analytical solution of Eqs. (7).

Let us obtain an analytical solution of the two-wave MB Eqs. (7) under the condition of zero initial inversion for a periodic $\tilde{\rho}(\xi)$ with a period $d' = \lambda'/2$. Results of the numerical simulation let us search an automodel solution in the form

$$\Omega^-(\xi, \tau) = 0, \quad \Omega^+(\xi, \tau) = \Omega^+(\varphi), \quad (21)$$

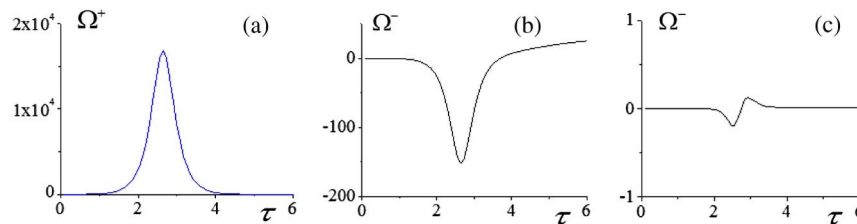


Fig. 2. Dependencies on the nondimensional time coordinate $\tau = t/\tau_c$ of wave amplitudes at the left boundary of the structure $\xi = 0$ obtained using numerical simulation of the MB Eqs. (7): (a) forward wave $\Omega^+(\xi = 0; \tau)$ (arb. units), (b) backward wave $\Omega^-(\xi = 0; \tau)$ in the case of $n_0 = -1$, and (c) backward wave $\Omega^-(\xi = 0; \tau)$ in the case of $n_0 = 0$.

which is a solution in the form of a pulse having an arbitrary but invariant profile which is defined by initial conditions. Then

$$\Omega_\xi^\pm = \frac{1}{v\tau_p} \Omega_\varphi^\pm, \quad \Omega_\tau^\pm = -\frac{1}{\tau_p} \Omega_\varphi^\pm, \quad (22)$$

where the subscript φ indicates a partial derivative with respect to φ . Representing P as $P = P_1 + iP_2$, where $P_{1,2}$ are real functions, reduce Eqs. (7b) and (7c) to the Bloch equations containing P_1 , P_2 , and n ,

$$\begin{aligned} P_{1\tau} &= n\Omega^+ \cos k'\xi, \\ P_{2\tau} &= n\Omega^+ \sin k'\xi, \\ n_\tau &= -\Omega^+(P_1 \cos k'\xi + P_2 \sin k'\xi). \end{aligned} \quad (23)$$

It is easy to check that the Eqs. (23) exhibit the conservation law

$$P_1^2 + P_2^2 + n^2 = 1 \quad (24)$$

for the length of the Bloch vector $\mathbf{R} = (P_1, P_2, n)$, $|\mathbf{R}|^2 = 1$ [Fig. 4(a)].

The Bloch Eqs. (23) are equivalent to one vector equation

$$\mathbf{R}_\tau = [\boldsymbol{\Omega}' \times \mathbf{R}], \quad (25)$$

where the torque vector is given by $\boldsymbol{\Omega}' = (\Omega_1, \Omega_2, \Omega_3)$:

$$\Omega_1 = -\Omega^+ \sin k'\xi, \quad \Omega_2 = \Omega^+ \cos k'\xi, \quad \Omega_3 = 0.$$

Thereby, the vector $\boldsymbol{\Omega}'$ lies in the plane formed by the axes P_1 and P_2 [Fig. 4(b)]. The vector \mathbf{R} rotates around $\boldsymbol{\Omega}'$ so that its end draws a circle, the Bloch vector itself by rotation draws a cone. The angle α between vectors \mathbf{R} and $\boldsymbol{\Omega}'$ is equal to $k'\xi$ at any time.

To solve the vector Eq. (25), let us pass on to the coordinate system with new axes P'_1 , P'_2 , and n' , rotated with respect to the old coordinate system by $\alpha = k'\xi$ around the axis n . Thereby, the axis P'_2 is directed along the vector $\boldsymbol{\Omega}'$ and the axis n' coincides with the axis n .

In the new coordinate system, we seek the solution in the form

$$P'_1 = \sin \alpha \cos \theta, \quad P'_2 = \cos \alpha, \quad n' = -\sin \alpha \sin \theta, \quad (26)$$

where $\theta = \theta(\xi, \tau)$ is an angle taken from the point A anticlockwise [Fig. 4(c)]. The circle drawn in the figure is a trajectory of

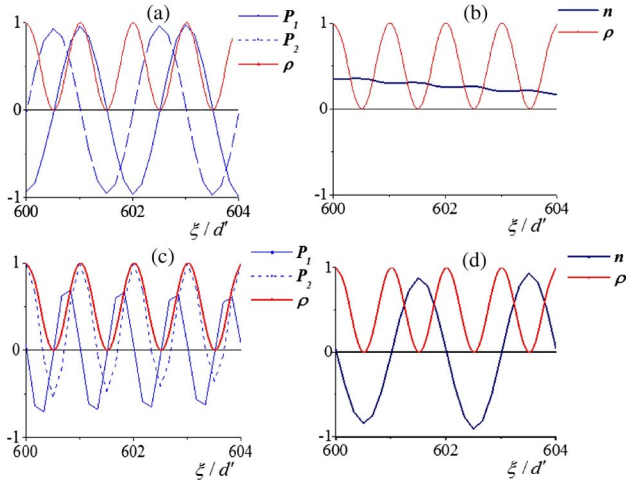


Fig. 3. Spatial dependencies of $P_1(\xi)$, $P_2(\xi)$, $n(\xi)$, and the function of resonant atom concentration $\tilde{\rho}(\xi)$ within the propagating pulse at some moment under condition (a), (b) $n_0 = -1$ and (c), (d) $n_0 = 0$. These dependencies have been obtained using numerical solving of the MB Eqs. (7); $\xi/d' = x/d$ is the spatial coordinate in units of the structure period d .

the end of the Bloch vector in the plane P'_1 , n' and its radius equals $R \sin \alpha$. Initially, an end of the Bloch vector is in the point A, $\theta(\xi; \tau = 0) = 0$.

Transition to the original coordinate system is accomplished by means of the rotation matrix

$$\begin{pmatrix} P_1 \\ P_2 \\ n \end{pmatrix} = \begin{pmatrix} \cos \alpha & -\sin \alpha & 0 \\ \sin \alpha & \cos \alpha & 0 \\ 0 & 0 & 1 \end{pmatrix} \begin{pmatrix} P'_1 \\ P'_2 \\ n' \end{pmatrix}. \quad (27)$$

Finally, introducing Eq. (26) into Eq. (27), we obtain

$$\begin{aligned} P_1 &= -(1/2) \sin 2\alpha(1 - \cos \theta), \\ P_2 &= \sin^2 \alpha \cos \theta + \cos^2 \alpha, \\ n &= -\sin \alpha \sin \theta. \end{aligned} \quad (28)$$

Introducing Eqs. (28) into the Bloch Eqs. (23), we get the connection between an angle θ and a propagating wave amplitude Ω^+ ,

$$\theta(\xi, \tau) = \int_{-\infty}^{\tau} \Omega^+(\xi, \tau') d\tau'. \quad (29)$$

As the mean atom dipole moment P [Eq. (28)] has the spatial phase $2\alpha = 2k'\xi$, the right-hand part of Eq. (7a),

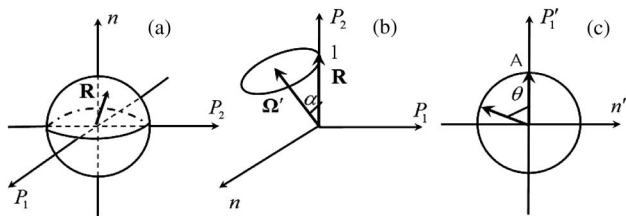


Fig. 4. (a) Bloch sphere. (b) Rotation of the Bloch vector \mathbf{R} around the vector Ω' under the condition of $\mathbf{R}(\xi; \tau = 0) = (0, 1, 0)$. (c) Trajectory of the Bloch vector end in the plane P'_1 , n' . Initially, the Bloch vector end is in the point A.

by averaging, becomes a zero value due to spatial phase mismatching between atom dipole moments and field wave. Zeroing of the right-hand part leads to suppression of the Bragg reflection $\Omega^-(\xi, \tau) = 0$ and to invariance of the propagating wave profile $\Omega^+(\xi, \tau) = \Omega^+(\varphi)$ while it passes through the RPC.

Finally, the solutions (21), (28), and (29) of the MB Eqs. (7) under the condition of zero initial inversion $n_0 = 0$ is

$$\begin{aligned} \Omega^+(\xi, \tau) &= \Omega^+(\varphi), \\ \Omega^-(\xi, \tau) &= 0, \\ P_1(\xi, \tau) &= -(1/2) \sin 2k'\xi[1 - \cos \theta(\xi, \tau)], \\ P_2(\xi, \tau) &= \sin^2 k'\xi \cos \theta(\xi, \tau) + \cos^2 k'\xi, \\ n(\xi, \tau) &= -\sin k'\xi \sin \theta(\xi, \tau). \end{aligned}$$

If the pulse area Eq. (29) is $\theta = 2\pi$, the state of excited atoms after pulse passing does not change because the Bloch vector is rotated for 2π by the pulse and then returns back to its initial state: $P_1 = 0$, $P_2 = 1$, $n = 0$. So a quasi-linear 2π pulse propagates in the Bragg structure. Each atom response is nonlinear because atom dipole moment and inversion have a nonlinear dependence on the field [Eq. (28)], but average resonant medium polarization is zero and pulse propagates as in a linear medium. Unlike a nonlinear GS, the form of the quasi-linear 2π pulse may be arbitrary but its area must be equal to 2π . The obtained analytical solution is in good agreement with numerical one (Fig. 5).

The analogous effect in the case of $n_0 = 0$ is also observed under incoherent initial pump when the dipole moment phases of resonant atoms are random in the initial moment of time. In this case, a pulse propagates also with velocity equal to the light velocity in a linear matrix without Bragg reflection.

Let us show that, in a continuous RPC, changing of resonant atom concentration profile can enlarge pulse intensity and simultaneously reduce its duration. For this purpose, we carry out numerical integration of the set of Eqs. (7) with the following initial conditions:

$$\begin{aligned} \Omega^\pm(\xi; \tau = 0) &= \Omega_0^\pm \operatorname{sech} \varphi, \\ P_1(\xi; \tau = 0) &= P_0 \operatorname{sech} \varphi \theta \varphi \cos k'\xi, \\ P_2(\xi; \tau = 0) &= P_0 \operatorname{sech} \varphi \theta \varphi \sin k'\xi, \\ n(\xi; \tau = 0) &= -1 + 2 \operatorname{sech}^2 \varphi, \\ \Omega^+(\xi = 0; \tau) &= 0, \quad \Omega^-(\xi = L; \tau) = 0. \end{aligned}$$

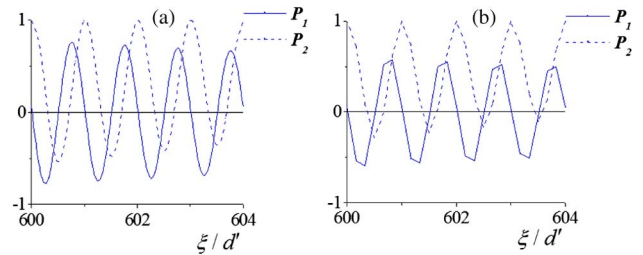


Fig. 5. Spatial dependencies $P_1(\xi)$ and $P_2(\xi)$ in the case of $n_0 = 0$: (a) the analytical solution, (b) the numerical solution. $\xi/d' = x/d$ is the spatial coordinate in units of the structure period d .

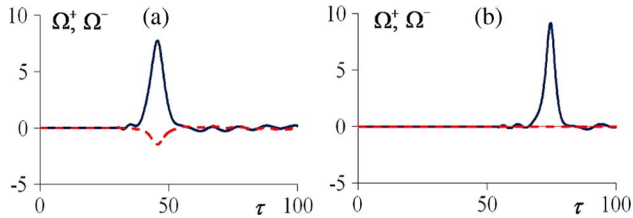


Fig. 6. Dependencies of amplitudes of the counterpropagating Bragg waves $\Omega^+(\tau)$ (continuous lines, arb. units) and $\Omega^-(\tau)$ (dotted lines, arb. units) on time τ calculated numerically by Eqs. (7): (a) at the input into the excited region $\xi/d' = 1400$ and (b) at the output of the structure $\xi/d' = 2200$.

We take the following resonant atom concentration profile:

$$\tilde{\rho}(\xi) = \sum_{m=0}^{L/d'} a \operatorname{sech}(ak'\xi) \tilde{\delta}(\xi - md'), \quad (30)$$

where function $\tilde{\delta}(\xi - md')$ equals 1 at $\xi \in (md' \pm d'/2)$ and zero at any other point.

Parameter a defines both a profile amplitude and a profile width. Thus, changing a , we conserve the number of resonant atoms within the period of the structure. The structure consists of two parts. Over 1400 periods in the beginning of the structure $a = 8$ and, as it is shown above, a soliton forms within this segment. The pulse velocity $v = 0.68$ and its duration $\tau_p = 0.46$. Then we slowly lessen an amplitude of the profile modulation [Eq. (30)] until the value $a = 2$ in the region of the length $\Delta L = 800d'$. The pulse accelerates to velocity 0.88, its forward wave amplitude increases, and the backward one becomes smaller. In Fig. 6, the dependencies of the counterpropagating Bragg wave amplitudes Ω^+ and Ω^- on time at the input of the excited region $\xi/d' = 1400$ and at the output of the structure ($\xi/d' = 2200$) are shown. Pulse compression at half height is nearly 40%; its intensity increase is also 40%. It is well seen from Fig. 6 that pulse amplitude increases not only due to pulse compression but and because of energy transfer from backward wave to the forward one. This effect appears within the linear photonic band gap since slow adiabatic pulse duration reduction keeps the pulse spectrum within the band gap. The band gap does not allow “linear radiation” to leave the pulse, even under changing of the soliton-like amplitude envelope profile. Due to nonlinearity of interaction, the radiation also does not stay in the structure in the form of a standing wave.

4. CONCLUSION

In conclusion, the theory of interaction of intensive coherent radiation with a continuous RPC having an arbitrary resonant atom concentration profile, developed in this paper, allows one to generalize some nonlinear effects (nonlinear Bragg reflection, gap soliton, super-radiance) obtained earlier in a discrete RPC to a wide class of the structures. Pulse dynamics in a continuous RPC is essentially influenced by the initial excitation of resonant atoms. If the atoms are not excited initially, radiation propagates in the form of the gap soliton of self-induced transparency while, in the case of zero initial inversion, the Bragg reflection for the 2π pulse is suppressed entirely and a backward wave does not exist. The pulse coherently propagates in the Bragg structure as a quasi-linear 2π pulse. The same coherent effect of a quasi-linear 2π pulse

propagation can also be observed in a homogeneous unmodulated medium. The possibility of compression of laser pulses is shown under slow changing of the amplitude of concentration of resonant atoms in a continuous RPC. It can be expected that the well-designed profile of the periodic concentration of resonant atoms, allowing solitons to have quite small velocity, may help even more effective pulse compression and intensity increase. The possibility of pulse parameter control using changing of the initial conditions and structure profile is of a great applied interest.

ACKNOWLEDGMENTS

This work was partially supported by the Russian Foundation for Basic Research, Grant Nos. 13-02-00300 and 11-02-01470.

REFERENCES

1. Yu. S. Kivshar and G. P. Agrawal, *Optical Solitons: From Fibers to Photonic Crystals* (Academic, 2003).
2. K. Busch, G. Von Freymann, S. Linder, S. Mingaleev, L. Tkeshelashvili, and M. Wegener, “Periodic nanostructures for photonics,” *Phys. Rep.* **444**, 101–202 (2007).
3. Y. V. Kartashov, B. A. Malomed, and L. Torner, “Solitons in nonlinear lattices,” *Rev. Mod. Phys.* **83**, 247–305 (2011).
4. B. I. Mantsyzov and R. N. Kuzmin, “Coherent interaction of light with a discrete periodic resonant medium,” *Zh. Eksp. Teor. Fiz.* **91**, 65–77 (1986) [*Sov. Phys. JETP* **64**, 37–44 (1986)].
5. A. Kozhokin and G. Kurizki, “Self-induced transparency in Bragg reflectors: gap solitons near absorption resonators,” *Phys. Rev. Lett.* **74**, 5020–5023 (1995).
6. N. Akozbek and S. John, “Self-induced transparency solitary waves in a doped nonlinear photonic band gap material,” *Phys. Rev. E* **58**, 3876–3895 (1998).
7. E. V. Kazantseva and A. I. Maimistov, “Polaritonic gap-soliton propagation through a wide defect in a resonantly absorbing Bragg grating,” *Phys. Rev. B* **79**, 033812 (2009).
8. R. A. Vlasov and A. M. Lemeza, “Bistable moving optical solitons in resonant photonic crystal,” *Phys. Rev. A* **84**, 023828 (2011).
9. W. Chen and D. L. Mills, “Gap solitons and the nonlinear optical response of superlattices,” *Phys. Rev. Lett.* **58**, 160–163 (1987).
10. D. N. Christodoulides and R. I. Joseph, “Slow Bragg solitons in nonlinear periodic structures,” *Phys. Rev. Lett.* **62**, 1746–1749 (1989).
11. A. B. Aceves and S. Wabnitz, “Self-induced transparency solitons in nonlinear refractive periodic media,” *Phys. Lett. A* **141**, 37–42 (1989).
12. J. T. Mok, C. M. deSterke, and B. J. Eggleton, “Delay-tunable gap-soliton-based slow-light system,” *Opt. Express* **14**, 11987–11996 (2006).
13. J. T. Mok, C. M. deSterke, I. C. Littler, and B. J. Eggleton, “Dispersionless slow light using gap soliton,” *Nat. Phys.* **2**, 775–780 (2006).
14. C. Conti, S. Trillo, and G. Assanto, “Doubly resonant Bragg simultons via second-harmonic generation,” *Phys. Rev. Lett.* **78**, 2341–2344 (1997).
15. C. Conti, G. Assanto, and S. Trillo, “Self-sustained trapping mechanism of zero-velocity parametric gap-solitons,” *Phys. Rev. E* **59**, 2467–2470 (1999).
16. B. I. Mantsyzov and R. A. Silnikov, “Unstable excited and stable oscillating gap 2π -pulses,” *J. Opt. Soc. Am. B* **19**, 2203–2207 (2002).
17. B. I. Mantsyzov, “Optical zoomeron as a result of beatings of the internal modes of a bragg soliton,” *JETP Lett.* **82**, 253–258 (2005).
18. B. I. Mantsyzov, I. V. Mel'nikov, and J. S. Aitchison, “Controlling light by light in a one-dimensional resonant photonic crystal,” *Phys. Rev. E* **69**, 055602 (2004).
19. W. N. Xiao, J. Y. Zhou, and J. P. Prineas, “Storage of ultrashort optical pulses in a resonantly absorbing Bragg reflector,” *Opt. Express* **11**, 3277–3288 (2003).
20. W. Xiao, “Trapping gap solitons in a resonant photonic crystal of finite length,” *Phys. Rev. E* **75**, 066610 (2007).

21. S. E. Svyakhovskiy, A. I. Maydykovsky, and T. V. Murzina, "Mesoporous silicon photonic structures of thousands of periods," *J. Appl. Phys.* **112**, 013106 (2012).
22. S. E. Svyakhovskiy, V. O. Kompanets, A. I. Mailykovskiy, T. V. Murzina, S. V. Chekalin, V. A. Bushuev, A. A. Skorynin, and B. I. Mantsyzov, "Observation of diffraction-induced laser pulse splitting in a photonic crystal," *Phys. Rev. A* **86** 013843 (2012).
23. B. I. Mantsyzov, E. V. Petrov, and M. V. Fedotov, "Gap soliton of self-induced transparency in periodic structure with arbitrary modulated density of resonant atoms," *Bull. Russ. Acad. Sci., Phys.* **70**, 167–173 (2006).
24. L. Allen and J. H. Eberly, *Optical Resonance and Two-Level Atoms* (Wiley, 1975).
25. F. Arecchi and E. Courtens, "Cooperative phenomena in resonant electromagnetic propagation," *Phys. Rev. A* **2**, 1730–1737 (1970).